

# GigaScience

## MetaPGN: a pipeline for construction and graphical visualization of annotated pangenome networks

--Manuscript Draft--

<b>Manuscript Number:</b>	GIGA-D-18-00147R1	
<b>Full Title:</b>	MetaPGN: a pipeline for construction and graphical visualization of annotated pangenome networks	
<b>Article Type:</b>	Research	
<b>Funding Information:</b>	National Natural Science Foundation of China (31601073)	Dr Junhua Li
<b>Abstract:</b>	<p>Pangenome analyses facilitate the interpretation of genetic diversity and evolutionary history of a taxon. However, there is an urgent and unmet need to develop new tools for advanced pangenome construction and visualization, especially for metagenomic data. Here we present an integrated pipeline, named MetaPGN, for graphically construction and visualization of pangenome networks from microbial genomes or metagenomes. Given isolate genomes or metagenomic assemblies coupled with a reference genome of the targeted taxon, MetaPGN generates a pangenome in a topological network, consisting of genes (nodes) and gene-gene genomic adjacencies (edges) of which biological information can be easily updated and retrieved. MetaPGN also includes a self-developed Cytoscape plugin for layout of and interaction with the resulting pangenome network, providing an intuitive and interactive interface for fully exploration of genetic diversity. We demonstrate the utility of MetaPGN by constructing Escherichia coli (E. coli) pangenome networks from five E. coli pathogenic strains and 760 human gut microbiomes respectively, revealing extensive genetic diversity of E. coli within both isolates and gut microbial populations. With the ability to extract and visualize gene contents and gene-gene physical adjacencies of a specific taxon from large-scale metagenomic data, MetaPGN provides advantages in expanding pangenome analysis to uncultured microbial taxa. MetaPGN is available at <a href="https://github.com/peng-ye/MetaPGN">https://github.com/peng-ye/MetaPGN</a>.</p>	
<b>Corresponding Author:</b>	Junhua Li, Ph.D. BGI shenzhen, guangdong CHINA	
<b>Corresponding Author Secondary Information:</b>		
<b>Corresponding Author's Institution:</b>	BGI	
<b>Corresponding Author's Secondary Institution:</b>		
<b>First Author:</b>	Ye Peng	
<b>First Author Secondary Information:</b>		
<b>Order of Authors:</b>	Ye Peng	
	Shanmei Tang	
	Dan Wang	
	Huanzi Zhong	
	Huijue Jia	
	Xianghang Cai	
	Zhaoxi Zhang	
	Minfeng Xiao	
	Huanming Yang	

	Jian Wang
	Karsten Kristiansen, professor
	Xun Xu
	Junhua Li, Ph.D.
<b>Order of Authors Secondary Information:</b>	
<b>Response to Reviewers:</b>	We appreciate the time and efforts by the editors and referees in reviewing this manuscript. We thank the referees for their helpful comments and suggestions. The manuscript has now been carefully revised to address all their concerns (major revisions are denoted in blue). In order to try the double-blind peer reviewing process, author information, authors' contribution and acknowledgement parts have been removed from the text. We believed that the revised version should meet the journal publication requirements. See the supplementary file named PBP_responses_to_editor_and_reviewers.docx for detailed point-by-point responses.
<b>Additional Information:</b>	
<b>Question</b>	<b>Response</b>
Are you submitting this manuscript to a special series or article collection?	No
<b>Experimental design and statistics</b>  Full details of the experimental design and statistical methods used should be given in the Methods section, as detailed in our <a href="#">Minimum Standards Reporting Checklist</a> . Information essential to interpreting the data presented should be made available in the figure legends.  Have you included all the information requested in your manuscript?	Yes
<b>Resources</b>  A description of all resources used, including antibodies, cell lines, animals and software tools, with enough information to allow them to be uniquely identified, should be included in the Methods section. Authors are strongly encouraged to cite <a href="#">Research Resource Identifiers</a> (RRIDs) for antibodies, model organisms and tools, where possible.  Have you included the information requested as detailed in our <a href="#">Minimum Standards Reporting Checklist</a> ?	Yes

<p><b>Availability of data and materials</b></p> <p>All datasets and code on which the conclusions of the paper rely must be either included in your submission or deposited in <a href="#">publicly available repositories</a> (where available and ethically appropriate), referencing such data using a unique identifier in the references and in the “Availability of Data and Materials” section of your manuscript.</p> <p>Have you have met the above requirement as detailed in our <a href="#">Minimum Standards Reporting Checklist</a>?</p>	<p>No</p>
<p>If not, please give reasons for any omissions below.</p> <p>as follow-up to "<b>Availability of data and materials</b></p> <p>All datasets and code on which the conclusions of the paper rely must be either included in your submission or deposited in <a href="#">publicly available repositories</a> (where available and ethically appropriate), referencing such data using a unique identifier in the references and in the “Availability of Data and Materials” section of your manuscript.</p> <p>Have you have met the above requirement as detailed in our <a href="#">Minimum Standards Reporting Checklist</a>?</p> <p>"</p>	<p>We are uploading assembled contigs of 760 metagenomes used in this study to EBI and CNSA, and will provide accession numbers when it is done.</p>

[Click here to view linked References](#)

# MetaPGN: a pipeline for construction and graphical visualization of annotated pangenome networks

## Abstract

Pangenome analyses facilitate the interpretation of genetic diversity and evolutionary history of a taxon. However, there is an urgent and unmet need to develop new tools for advanced pangenome construction and visualization, especially for metagenomic data. Here we present an integrated pipeline, named MetaPGN, for construction and graphical visualization of pangenome network from either microbial genomes or metagenomes. Given either isolated genomes or metagenomic assemblies coupled with a reference genome of the targeted taxon, MetaPGN generates a pangenome in a topological network, consisting of genes (nodes) and gene-gene genomic adjacencies (edges) of which biological information can be easily updated and retrieved. MetaPGN also includes a self-developed Cytoscape plugin for layout of and interaction with the resulting pangenome network, providing an intuitive and interactive interface for full exploration of genetic diversity. We demonstrate the utility of MetaPGN by constructing *Escherichia coli* (*E. coli*) pangenome networks from five *E. coli* pathogenic strains and 760 human gut microbiomes respectively, revealing extensive genetic diversity of *E. coli* within both isolates and gut microbial populations. With the ability to extract and visualize gene contents and gene-gene physical adjacencies of a specific taxon from large-scale metagenomic data, MetaPGN provides advantages in expanding pangenome analysis to uncultured microbial taxa. MetaPGN is available at <https://github.com/peng-ye/MetaPGN>.

**Keywords:** pangenome, visualization, metagenomics

# Introduction

The concept of the pangenome, defined as the full complement of genes in a clade, was first introduced by Tettelin *et al.* in 2005 [1]. Pangenome analyses of a species now provide insights into core- and accessory-genome profiles, within-species genetic diversity, evolutionary dynamics and niche-specific adaptations. A number of methods and tools have to date been proposed for pangenome analysis on genomic or metagenomic data (Table 1).

Typical pangenome tools such as GET\_HOMOLOGUES [2] and PGAP [3], mainly focus on analyzing homologous gene families and calculating the core/accessory genes of a given taxon. However, these tools cannot provide the variations of gene-gene physical relationships. Tools like GenoSets [4], PGAT [5], PEGR [6], EDGAR [7], GenomeRing [8] and PanViz [9] are developed to generate a linear or circular presentation of compared genomes, which can indicate the physical relationships between genomic sequences or genes. However, in the linear or circular representations generated by these tools, the same homologous region is visualized multiple times and shown on separate input genomes. Hence, it will be difficult for users to track a homologous region among the input genomes, especially when there is a large number of homologous regions and input genomes.

Pangenomes built using *de Bruijn* graph, like SplitMEM [10] and a tool introduced by Baier *et al.* [11], partly solve the above problems. In the resulting graph generated by these tools, the complete pangenome is represented in a compact graphical representation such that the core/accessory status of any genomic sequences is immediately identifiable, along with the context of the flanking sequences. This strategy enables powerful topological analysis of the pangenome not possible from a linear/circular representation. Nevertheless, tools based on the *de Bruijn* graph algorithm can only construct a compact network comprised of core/accessory genomic sequences instead of genes, which means retrieving or updating functional information in downstream analysis will be difficult. Furthermore, these tools do not visualize the constructed *de Bruijn* graph and provide an interactive interface for users to explore the graph.

Moreover, all the above-mentioned tools analyze pangenomes via genomic data which require organisms isolated from the environment and cultured *in vitro*. Recent advances in metagenomics have led to a paradigm shift in pangenome studies from a limited quantity of cultured microbial

1  
2  
3  
4 genomes to large-scale metagenomic datasets containing huge potential for functional and  
5 phylogenetic resolution from the still uncultured taxa. Several existing tools dealing with  
6 metagenomic data are based on constructed pangenomes and cannot utilize the abundant gene  
7 resources contained in metagenomes to extend the pangenomes in question. For example,  
8 PanPhlAn [12], MIDAS [13], and a pipeline introduced by Delmont and Eren [14] maps reads  
9 onto a reference pangenome, to describe the pattern of the presence/absence of genes in  
10 metagenomes. As for another example, Kim *et al.* [15] clustered genes predicted from  
11 metagenomic contigs with *Bacillus* core genes for profiling the *Bacillus* species in the  
12 microbiomes. Recently, Farag *et al.* [16] aligned metagenome contigs with reference genomes for  
13 identification of “*Latescibacteria*” genomic fragments. Even though this strategy can theoretically  
14 recruit sequences not present in the reference genomes, it is likely to filter out “*Latescibacteria*”  
15 genomic fragments with structural variations compared to the reference ones. Furthermore, all  
16 these aforementioned methods using metagenomic data do not organize the pangenome using a  
17 network, which is essential for efficiently storage and visualization of pangenomes constructed  
18 from metagenomic data.  
19  
20  
21  
22  
23  
24  
25  
26  
27  
28  
29  
30  
31

32 Here, we introduce an integrated pipeline (MetaPGN) for network-based construction and  
33 visualization of prokaryotic pangenomes for both isolated genomes and metagenomes. Given  
34 genomic or metagenomic assemblies and a reference genome of a taxon of interest, MetaPGN  
35 derives a pangenome network for integrating genes (nodes) and gene-gene adjacencies (edges)  
36 belonging to a given taxon. MetaPGN also includes a specific Cytoscape plugin for layout of and  
37 interaction with the resulting pangenome network, providing an intuitive and interactive interface  
38 for the exploration of gene diversity. For example, in the visualized network in Cytoscape, users  
39 can specify gene annotations, customize the appearance of nodes and edges, and search and  
40 concentrate on genes of certain functions. We applied MetaPGN on assemblies from five  
41 pathogenic *E. coli* strains and 760 human gut microbiomes respectively, with *E. coli* K-12 substr.  
42 MG1655 (*E. coli* K-12) being the reference genome. Our results showed that by taking gene  
43 adjacency into account and visualizing the pangenome network in a well-organized manner,  
44 MetaPGN can assist in illustrating genetic diversity in genomic or metagenomic assemblies  
45 graphically and conveniently.  
46  
47  
48  
49  
50  
51  
52  
53  
54  
55  
56  
57  
58  
59  
60  
61  
62  
63  
64  
65

# Results

**General workflow.** MetaPGN accepts genome or metagenome assemblies as input (query assemblies) and requires a reference genome for recruitment of the query assemblies and as the skeleton of the pangenome network. The MetaPGN pipeline can be divided into two main parts: (i) construction of a pangenome network comprised of representative genes, including gene prediction, gene redundancy elimination, gene type determination, pairwise gene adjacency extraction, assembly recruitment (for metagenomic assemblies), and pangenome network generation, and (ii) visualization of the pangenome network in an organized way, where nodes represent genes and edges indicate gene adjacencies, in Cytoscape [17] with a self-developed plugin (Fig. 1, Fig. S1, and Methods). From the resultant pangenome network, the degree of similarity among homologous genes, as well as their genomic context is easily visible. Of note, users can further add and update annotation for nodes and edges in the networks, based on which elements of interest can be accessed conveniently.

**Pangenome network of 5 pathogenic *Escherichia coli* genomes.** In order to demonstrate its potential in studying microbial genetic diversity and phenotype-genotype relationship, we first applied MetaPGN on genomes of 5 pathogenic *E. coli* isolates, *E. coli* O26:H11 str. 11368, *E. coli* O127:H6 E2348/69, *E. coli* O157:H7 str. EDL933, *E. coli* O104:H4 str. 2011C-3493 and *E. coli* 55989. A commensal *E. coli* strain, K-12 substr. MG1655 (Supplementary Table S1) was chosen as the reference genome in this instance and in all examples shown below.

A pangenome network consisting of 9,161 nodes and 11,788 edges (Supplementary Table S3, Supplementary File 2) was constructed and visualized (Methods). Based on the well visualized pangenome network along with functional annotation, we can now graphically observe the extent of variations of certain genes, as well as their genomic context. For example, when focusing on a cluster of flagellar genes (Fig. 2a), we found that *fliC* sequences encoding the filament structural protein (H-antigen) and *fliD* sequences encoding the filament capping protein are highly divergent with nucleotide sequence identity < 95% and/or overlap < 90% among these *E. coli* strains (See Methods). In contrast, four genes encoding chaperones (*fliS*, *fliT*, *fliY*, *fliZ*) and a gene related to regulation of expression of flagellar components (*fliA*) are conserved (nucleotide sequence identity

1  
2  
3  
4  $\geq 95\%$  and overlap  $\geq 90\%$ ) over all the *E. coli* strains investigated. A gene (270bp) encoding a  
5  
6 hypothetical protein is uniquely presented between *fliC* and *fliD* in *E. coli* O157:H7 str. EDL933.

7  
8 In a fimbria protein-related gene cluster, compared to the reference *E. coli* strain, all the 5  
9  
10 pathogenic strains possess several genes located between two conserved genes encoding an outer  
11  
12 membrane protein and a regulatory protein, and *E. coli* O127:H6 E2348/69 uniquely exhibits more  
13  
14 genes encoding proteins of unknown functions (Fig. 2b).

15  
16 For a gene cluster responsible for the biosynthesis of lipopolysaccharides (LPS), *E. coli*  
17  
18 O127:H6 E2348/69 shares three genes with the reference strain that differentiate from the other 4  
19  
20 pathogenic strains (Fig. 2c). For another gene cluster of related function, the *E. coli* O127:H6  
21  
22 E2348/69 also shows a strain-specific duplication event of two genes involved in colanic acid (CA)  
23  
24 synthesis (*wcaH* and *wcaG*, denoted by a purple dash line in Fig. 2d). It has been demonstrated  
25  
26 that CA can modify lipopolysaccharide (LPS) generating a novel form ( $M_{LPS}$ ) which may enhance  
27  
28 survival of *E. coli* in different ways [18]. The two *wcaH* genes in *E. coli* O127:H6 E2348/69, may  
29  
30 even though they share high similarity (99.1% identity) confer the strain with different functional  
31  
32 potentials for CA formation and thereby novel survival mechanisms.

33  
34 In addition, the German outbreak *E. coli* O104:H4 str. 2011C-3493 shares identical nodes and  
35  
36 edges in the flagellar-related gene cluster (Fig. 2a) and the O antigen-related gene cluster with a  
37  
38 historical *E. coli* 55989 (Fig. 2d), suggesting a close  
39  
40 evolutionary relationship between these strains as previously reported [19,20].

41  
42 These results demonstrate the feasibility of MetaPGN for construction and visualization of  
43  
44 microbial pangenomes in an organized way. Moreover, by involving genomic adjacency and  
45  
46 offering easy-to-achieve biological information, MetaPGN provides a convenient way to assist  
47  
48 biologists in exposing genetic diversity for genes of interest among the organisms under study.

49  
50 **Pangenome network of *E. coli* in 760 metagenomes.** Moving beyond surveying the pangenome  
51  
52 network of isolate genomes, we applied MetaPGN in metagenomic datasets to interrogate the *E.*  
53  
54 *coli* pangenome network on a grander scale. Assemblies of 760 metagenomes sequenced in the  
55  
56 Metagenomics of the Human Intestinal Tract (MetaHIT) project [21–24] were collected, which  
57  
58 contained 8,096,991 non-redundant genes with annotations [24]. As metagenome assemblies are  
59  
60 from varied taxa, it is necessary to recruit assemblies of the targeted taxon before construction of  
61  
62 the pangenome network. In this study, metagenome assemblies were recruited using a gene  
63  
64  
65



1  
2  
3  
4 alignment-based strategy, which was assessed with mock datasets (Methods). With the recruited  
5 assemblies, a pangenome network consisting of 9,406 nodes and 14,676 edges (Supplementary  
6 Table S3, Supplementary File S3) was generated and visualized after refinement (Methods).  
7  
8

9  
10 Based on annotation, we first searched flagellin-related genes in this network. We found that  
11 the pattern of adjacencies among these genes was similar to that in the pangenome network of the  
12 5 pathogenic *E. coli* genomes: *fliC* and *fliD* are hypervariable while *fliT*, *fliY*, *fliZ* and *fliA* are very  
13 conserved among these 760 samples. However, some genes of unknown function locate between  
14 *fliC* and *fliA* (Fig. 3a), instead of between *fliC* and *fliD* in the pangenome network of the 5  
15 pathogenic *E. coli* strains (Fig 2a).  
16  
17  
18  
19  
20

21 We then investigated mobile genetic elements (MGEs) in this pangenome network, as they can  
22 induce various types of genomic rearrangements[25]. Of the 362 nodes (~4%) annotated as MGE-  
23 related (according to Cluster of Orthologous Groups annotation done in reference [24]), many were  
24 flanked by shared genes on different *E. coli* genomes. In a region of the network, a gene cluster  
25 containing MGEs is query-specific, indicating there might be genomic rearrangements caused by  
26 strain-specific MGEs within the *E. coli* species (Fig. 3b). In another part of the network harboring  
27 MGEs, we observed that several branches of non-MGE genes are inserted in between two MGEs,  
28 which may imply a mutation hotspot within the region, or the existence of MGEs as yet  
29 undescribed (Fig. S1).  
30  
31  
32  
33  
34  
35  
36  
37

38 Application of MetaPGN in large-scale metagenomic data generated an *E. coli* pangenome  
39 network that might hardly be constructed from isolated genomes. As demonstrated here, the  
40 assembly-recruitment based, well-organized and visualized pangenome network can greatly  
41 expand our understanding in the genetic diversity of a taxon, although further efforts in  
42 bioinformatic and experimental analyses are needed to verify and extend these findings.  
43  
44  
45  
46  
47  
48  
49

50 **Assessment of pangenome networks derived from metagenomes.** Affected by the complexity  
51 of microbial communities, limitations in sequencing platforms and imperfections of bioinformatic  
52 algorithms, a genomic sequence of an organism is frequently split into dozens of assemblies when  
53 assembled from metagenomic reads. Due to this nature, a pangenome network recovered from a  
54 limited number of assemblies is likely to be segmented compared to a complete genome. To  
55 propose a minimum size of assemblies for getting an approximately complete connected  
56  
57  
58  
59  
60  
61  
62  
63  
64  
65

1  
2  
3  
4 pangenome network, we assessed the completeness of *E. coli* pangenome networks derived from  
5 varying size of recruited assemblies (Methods). As shown in Fig. 4, the count of connected  
6 subnetworks drops dramatically with the total length of recruited assemblies increasing from 5 Mb  
7 to 50 Mb (roughly from 1 × to 10 × of a *E. coli* genome), then barely changes even when using  
8 all recruited assemblies of the dataset (215 Mb, from 760 samples). Based on this analysis, a  
9 minimum size of recruited assemblies 10-fold of the studied genome is required to generate a  
10 relatively intact pangenome network when constructed from metagenomes.  
11  
12  
13  
14  
15  
16  
17  
18

## 19 Discussion

20  
21  
22 Since first coined more than a decade ago, pangenome analysis has provided a framework for  
23 studying the genomic diversity within a species. Current methods for pangenome analyses mainly  
24 focus on gene contents but ignore their genomic context, as well as having shortages in pangenome  
25 visualization. Besides, available methods are usually designed for genomic data and not capable  
26 of constructing pangenomes from metagenomics data. To fill these gaps, our MetaPGN pipeline  
27 takes genome or metagenome assemblies as input, uses gene contents as well as pairwise gene  
28 adjacency to generate a compact graphical representation for the gene network based on a reference  
29 genome, and visualizes the network in Cytoscape with a self-developed plugin (Fig. 1, Fig. S2).  
30  
31  
32  
33  
34  
35  
36  
37

38 From the two MetaPGN-derived *E. coli* pangenome networks, we can directly observe the  
39 diversity of genes among the five pathogenic *E. coli* strains and 760 human gut microbiomes with  
40 respect to the reference genome. For instance, in the pangenome network for the 5 pathogenic *E.*  
41 *coli* strains, we found that nucleotide sequences of the *fliC* gene which carries H-antigen specificity  
42 were highly divergent among the *E. coli* assemblies (Fig. 2a). These *fliC* sequences were more  
43 varied in the 760 human gut microbiomes (Fig. 3a). In addition, genes for synthesis of O-antigen  
44 and outer membrane protein showed a great diversity in the pangenome network of the 5 *E. coli*  
45 strains (Fig. 2c, Fig. 2d). These results are in agreement with previous findings on H-antigen  
46 specificity related genes [26–28] and O-antigen related genes [29,30]. We also showed that when  
47 gene adjacency is incorporated into the construction and visualization of pangenomes, locations  
48 of genes of unknown function are identified, which may be helpful for the inference of their  
49 biological functions. For example, in both the two pangenome networks, we found genes of  
50 unknown function locating between the *fliC* gene and other flagellin-related genes (Fig. 2a, located  
51  
52  
53  
54  
55  
56  
57  
58  
59  
60  
61  
62  
63  
64  
65

1  
2  
3  
4 between *fliC* and *fliD*, Fig. 3a, and located between *fliC* and *fliA*), indicating that these functionally  
5 unknown genes may play a role in flagellin biosynthesis [31], although further experimental trials  
6 are needed to prove this point. Additionally, from the pangenome network of the five *E. coli* strains,  
7 we observed a variation in *E. coli* O127:H6 E2348/69, which was shown to stem from a duplication  
8 event of two genes involved in colanic acid synthesis (*wcaH* and *wcaG*, Fig 2d). This finding  
9 indicates that knowledge of genomic adjacency may also shed light on structural variations among  
10 the input assemblies. If extended, genomic adjacency may further help in finding possible  
11 functional sequences which are associated with structural variations, as Delihias [32] and Wang *et*  
12 *al.* [33] reported on repeat sequences concentrated at the breakpoints of structural variations.  
13 Studying genomic adjacency can also improve the discovery of potential functional modules, as  
14 Doron *et al.* [34] systematically discovered bacterial defensive systems by examining gene  
15 families enriched next to known defense genes in prokaryotic genomes. These examples illustrate  
16 the value of including gene adjacencies in visualizing a pangenome to retrieve biological  
17 information. Although the examples shown in this study use the genome of a commensal *E. coli*  
18 strain for assembly recruitment and network arrangement, users can specify the reference genome  
19 when applying MetaPGN. Epidemiologists can use MetaPGN to compare assemblies of outbreak  
20 strains or viruses, such as *Vibrio cholerae* or Ebola virus, with those of some well-studied  
21 pathogenic strains to find novel variations involved in pathogenesis, which may further provide  
22 candidate targets for drug and vaccine design [35,36].

23  
24  
25  
26  
27  
28  
29  
30  
31  
32  
33  
34  
35  
36  
37  
38  
39  
40 Genomic variants of intestinal bacteria were found to be correlated with diseases. As one  
41 example, among the common members of the normal colonic microbiota, *Bacteroides fragilis* (*B.*  
42 *fragilis*), the inclusion of a pathogenicity island (BfPAI) distinguished enterotoxigenic strains  
43 (ETBF) from nontoxigenic ones (NTBF), by their ability to secrete a zinc-dependent  
44 metalloprotease toxin that can induce inflammatory diarrhea and even colon carcinogenesis  
45 [37,38]. As another example, Scher *et al.* performed shotgun sequencing on fecal samples from  
46 newly-onset untreated rheumatoid arthritis (NORA) patients and healthy individuals, and  
47 identified several NORA-specific *Prevotella copri* genes [39]. Hence, pangenome networks built  
48 from metagenomes of patients and healthy subjects may aid in detecting associated or causal  
49 genomic variants of a certain species.  
50  
51  
52  
53  
54  
55  
56  
57  
58  
59  
60  
61  
62  
63  
64  
65

1  
2  
3  
4 It should be noticed that, in this pipeline, we compare genes depending on nucleotide-level  
5 sequence identity and overlap: genes with  $\geq 95\%$  identity and  $\geq 90\%$  overlap are regarded as the  
6 same gene. However, genes sharing the same function may not satisfy this criterion ( $\geq 95\%$  identity  
7 and  $\geq 90\%$  overlap), and protein encoded by these genes may exhibit more similarity due to  
8 different codon usage. Hence, in our future work, we intend to cluster genes by comparing their  
9 nucleotide sequences as well as the amino acid sequences. Furthermore, the current MetaPGN  
10 pipeline does not consider other genomic features or physical distances between genes in  
11 constructing the pangenome network. Thus, differences in other genomic features such as  
12 ribosomal binding site (RBS) sequences [40,41] and distances between the RBS and start codons  
13 [42] may result in distinct phenotypes. Accordingly, users may include such information in  
14 analyzing pangenome networks.  
15  
16  
17  
18  
19  
20  
21  
22  
23

24  
25 To conclude, MetaPGN enables direct illustration of genetic diversity of a species in pangenome  
26 networks, improving understanding of genotype-phenotype relationships and evolutionary history.  
27  
28  
29

## 30 31 Methods

32  
33 **Pangenome network construction in MetaPGN.** First, gene prediction of query assemblies is  
34 performed using MetaGeneMark (Version 2.8) [43]. In order to eliminate redundancy, the resultant  
35 genes are clustered by CD-HIT (Version 4.5.7) [44] with identity  $\geq 95\%$  and overlap  $\geq 90\%$ , and  
36 genes in a same cluster are represented by the longest sequence of the cluster which is termed the  
37 representative gene. Representative genes of all clusters are subsequently aligned against genes on  
38 the given reference genome using BLAT (Version 34) [45]. From the alignment result, genes  
39 shared between the representative gene set and the reference gene set with identity  $\geq 95\%$   
40 and overlap  $\geq 90\%$  are defined as ‘shared genes’. The remaining representative and reference genes  
41 other than those shared genes are defined as ‘query-specific genes’ and ‘reference-specific genes’,  
42 respectively. Pairwise gene physical adjacency of representative genes on the query assemblies  
43 and of reference genes are then extracted, and status for each adjacency of being ‘shared’, ‘query-  
44 specific’, or ‘reference-specific’ is determined. Finally, based on the recruited assemblies and the  
45 reference genome, an initial pangenome network is generated: each node stands for a reference  
46 gene or a representative gene on the recruited assemblies; two nodes are connected by an edge if  
47 they are physically adjacent on the recruited assemblies or on the reference genome. The weight  
48  
49  
50  
51  
52  
53  
54  
55  
56  
57  
58  
59  
60  
61  
62  
63  
64  
65

1  
2  
3  
4 of a node or an edge denotes its occurrence frequency on all of the recruited assemblies and the  
5 reference genome.  
6  
7  
8  
9

10 **Pangenome network visualization in MetaPGN.** The following preprocessing work on the  
11 initial pangenome network was implemented before visualization: 1. The initial pangenome  
12 network was refined by removing isolated networks (networks not connected with the backbone)  
13 and tips (nodes only connected with another node); 2. Nodes and edges were added with some  
14 extra attributes, such as the status of the nodes and edges (query-specific, reference-specific or  
15 shared), whether the genes for the nodes were phage-, plasmid-, CRISPR- related genes and so on  
16 (**Supplementary Table S3**). Users can specify the attributes of nodes and edges according to their  
17 own datasets.  
18  
19  
20  
21  
22  
23  
24

25 We then used a self-developed Cytoscape plugin to visualize the pangenome network in an  
26 organized way (**Supplementary Text 2** in **Supplementary File S1** illustrates how to install and use  
27 the plugin in Cytoscape). Our algorithm for organizing nodes in the network is as follows:  
28  
29  
30

- 31 1. Construct a circular skeleton for the pangenome network with shared nodes and reference-  
32 specific nodes, according to positions of their related reference genes on the reference genome.  
33 If there are two or more representative genes similar to the same reference gene ( $\geq 95\%$  identity  
34 and  $\geq 90\%$  overlap), use one of these representative genes to construct the skeleton and place  
35 the others on both sides of the skeleton in turn (**Fig. S2 a**).  
36  
37  
38  
39  
40
- 41 2. Arrange query-specific nodes region by region, including,
  - 42 2.1. Select query-specific nodes in a region spanning less than 30 nodes in the skeleton  
43 (see **Supplementary Text 3** in **Supplementary File S2** for more details).  
44  
45
  - 46 2.2. Arrange these query-specific nodes as follows,
    - 47 i. For those that directly link with two nodes on the skeleton, place them on the bisector  
48 of the two skeleton nodes. If there are two or more query-specific nodes directly  
49 linking with the same pair of nodes on the skeleton, place them on both sides of the  
50 bisector of these pair of skeleton nodes in turn (**Fig. S2 b**).  
51  
52  
53  
54
    - 55 ii. Among the remaining nodes, for those that directly link with two placed nodes, place  
56 them on the bisectors of the placed ones. Iterate this step for five times (**Fig. S2 c**).  
57  
58  
59  
60  
61  
62  
63  
64  
65

- 1  
2  
3  
4       iii.     For the remaining nodes, place them into an arc without moving the placed nodes (Fig.  
5               S2 d), or else place them one by one starting near a placed node (Fig. S2 e).  
6  
7  
8  
9

10   **Construction and visualization of the 5-*E. coli*-genome pangenome network.** Genes were  
11 extracted from the complete genome for each strain (Supplementary Table S1). With *E. coli* K-12  
12 as the reference, a pangenome network was generated for these five *E. coli* strains using our  
13 MetaPGN tool. In the visualization of this pangenome network, we used green, blue and red color  
14 to denote a reference-specific, shared, and query-specific node or edge, respectively, and specified  
15 sizes of nodes and widths of edges with their occurrence frequency in the input genomes.  
16  
17  
18  
19  
20  
21  
22  
23

24   **Assessment of the gene alignment-based assembly recruitment strategy.** A gene alignment-  
25 based strategy was used for recruitment of metagenome assemblies in this study, which considers  
26 1) the count of genes on an assembly ( $c$ ), and 2) the ratio of the number of shared genes (designated  
27 as aforementioned) on an assembly to the total number of genes on that assembly ( $r$ ).  $c = 3$  paired  
28 with  $r = 0.5$ , requiring at least 3 genes including 2 shared genes containing in an assembly, was  
29 chosen for recruitment of metagenome assemblies in this study.  
30  
31  
32  
33  
34  
35

36     5 mock metagenomic datasets were used to assess the performance of this strategy. Briefly,  
37 simulated reads of 60 bacterial genomes from 14 common genera (*Bifidobacterium*, *Clostridium*,  
38 *Enterobacter*, *Escherichia*, *Haemophilus*, *Klebsiella*, *Lactobacillus*, *Neisseria*, *Pseudomonas*,  
39 *Salmonella*, *Shigella*, *Staphylococcus*, *Streptococcus*, *Yersinia*) present in the human gut  
40 (Supplementary Table S1), including the 5 pathogenic *E. coli* strains mentioned above and 10  
41 strains from *E. coli*-closely-related species (*Enterobacter aerogenes*, *Enterobacter cloacae*,  
42 *Escherichia albertii*, *Escherichia fergusonii*, *Klebsiella oxytoca*, *Klebsiella pneumoniae*, *Shigella*  
43 *boydii*, *Shigella sonnei* and *Salmonella enterica*), were generated by iMESSi [46]. Each dataset  
44 was simulated at the same complexity level with 100 million (M) 80bp paired-end reads of 12  
45 strains from 11-12 different genera, including 2 strains of closely related species to *E. coli*, and the  
46 relative abundances of strains were assigned by the broken-stick model (Supplementary Table S2).  
47 Simulated reads were first independently assembled into assemblies by SOAPdenovo2 in each  
48 dataset [43], with an empirical k-mer size of 41. Genes were then predicted on assemblies longer  
49  
50  
51  
52  
53  
54  
55  
56  
57  
58  
59  
60  
61  
62  
63  
64  
65

1  
2  
3  
4 than 500bp using MetaGeneMark [42] (default parameters were used except the minimum length  
5 of genes was set as 100bp).  
6  
7

8 Assemblies of each mock dataset were first aligned against the 5 pathogenic *E. coli* reference  
9 genomes by BLAT [45]. Those assemblies that have an overall  $\geq 90\%$  overlap and  $\geq 95\%$  identity  
10 with the reference genomes were considered as *E. coli* genome-derived (traditional genome  
11 alignment-based strategy). Those *E. coli* genome-derived assemblies containing at least three  
12 genes (i.e., containing at least two edges) were recruited for construction of a reference pangenome  
13 network (RPGN). A query pangenome network (QPGN) was then generated from assemblies  
14 selected by the gene alignment-based strategy with  $c = 3$  and  $r = 0.5$  as described above.  
15  
16  
17  
18  
19  
20  
21

22 Accuracy of query assembly recruitment was assessed, in respect of conformity and divergence  
23 between the RPGN with the QGPN (Supplementary Text 4 and 5 in Supplementary File S2). The  
24 result showed that the QPGN recovered 84.3% of node and 84.7% of edge in the RPGN, while  
25 falsely included 1.1% of node and 2.2% of edge, which demonstrated the high accuracy of the  
26 gene alignment-based strategy for recruitment of metagenome assemblies.  
27  
28  
29  
30  
31  
32  
33

34 **Construction and visualization of the 760-metagenome pangenome network.** Assemblies and  
35 representative genes of the 760 metagenomes generated in Reference [24] were used here, since  
36 they were produced using identical methods and parameter settings in this study. A pangenome  
37 network was generated following steps described above, again using *E. coli* K-12 as the reference,  
38 and  $c = 3$ ,  $r = 0.5$  for assembly recruitment. The resulting pangenome network was visualized in  
39 the same way as visualizing the 5-*E. coli*-genome pangenome network.  
40  
41  
42  
43  
44  
45  
46  
47

48 **Analysis of subnetworks comprising a pangenome network.** 10-700 metagenomes were  
49 randomly sampled from the above-mentioned 760 metagenomes. For each sub-dataset, a  
50 pangenome network was constructed after assembly recruitment using *E. coli* K-12 as the  
51 reference genome. For each pangenome network, reference-specific edges were removed before  
52 counting the number of subnetworks. Only sub-datasets with a size of recruited assemblies greater  
53 than 5 Mb were used to generate the scatterplot, in which a curve with 95% confidence intervals  
54 was fitted by the 'loess' smoothing method in R [47].  
55  
56  
57  
58  
59  
60  
61  
62  
63  
64  
65

## Computational resources and runtime

Timings for major steps of the MetaPGN pipeline are shown below. Tests were run on a single CPU of an Intel Core Processor (Broadwell) processor with 64 GB of RAM, without otherwise specified. The timings were CPU time including parsing input and writing outputs (h for hours, m for minutes, and s for seconds).

The average time for gene prediction for a mock metagenome was 7s, and it varies depending on the size of a metagenome. The time for redundancy elimination of genes using CD-HIT [44] was 1m 44s for the 5 *E. coli* stains, 50m 19s for the 5 mock datasets. For the 760 metagenomes, to perform redundancy elimination parallelly, we divided all genes into 200 sections, which resulted in 20,101 [ $N = (n + 1) \times (n \div 2) + 1, n = 200$ ] clustering tasks, and then submitted each task onto available machines in a high-performance computing cluster. The dividing step took 20m 4s with a peak memory usage of 10GB in the local machine, and the average time for a clustering task was 44m with taking less than 3GB of RAM, consuming total time of 14,814h. The time for recognizing the status (reference-specific, query-specific or shared) for nodes and edges was 10s for the 5 *E. coli* strains, 1m for the 5 mock datasets and 24m for the 760 metagenomes. Finally, the generation of the pangenome network took less than 1s for the 5 *E. coli* strains, less than 1s for the 5 mock datasets and 3m 35s for the 760 metagenomes.

**Data availability.** Genome sequence of 60 strains (including 5 *E. coli* strains) and the *E. coli* K-12 reference genome were downloaded from the National Center for Biotechnology Information (<ftp://ftp.ncbi.nlm.nih.gov/genomes/refseq/bacteria/>, Please refer to **Supplementary Table S1** for detailed information). Sequencing data of the 760 metagenomes were previously generated in the Metagenomics of the Human Intestinal Tract (MetaHIT) project [21–24], and assemblies of these 760 metagenomes are deposited at EBI under PRJEB28245. The MetaPGN pipeline, related manuals and Cytoscape session files for *E. coli* pangenome networks derived from five pathogenic *E. coli* strains and from 760 metagenomes are available on Github (<https://github.com/pengye/MetaPGN>) and SciCrunch (SCR\_016454).



# List of Figures

**Figure 1.** An Overview of the MetaPGN pipeline: from assemblies to a pangenome network. Gene prediction is performed on query assemblies. The resulting genes are clustered, after which genes in the same cluster are represented by the longest sequence of this cluster called the representative gene (node a-g). All these representative genes are then aligned against genes on the given reference genome. From the alignment result, genes shared between the representative gene set and the reference gene set are defined as ‘shared’ genes (blue). The remaining representative and reference genes other than those shared genes are defined as ‘query-specific’ genes (red) and ‘reference-specific’ genes (green), respectively. Pairwise gene physical adjacency of representative genes on the query assemblies and of reference genes are then extracted, and status for each adjacency of being ‘shared’ (blue), ‘query-specific’ (red), or ‘reference-specific’ (green) is determined. Finally, based on the recruited assemblies and the reference genome, a pangenome network is generated: each node stands for a reference gene or a representative gene on the recruited assemblies; two nodes are connected by an edge if they are physically adjacent on the recruited assemblies or the reference genome. The weight of a node or an edge is its occurrence frequency on all of the recruited assemblies and the reference genome (Methods). The pangenome network is then visualized in Cytoscape with a self-developed plugin (Methods) for a better arrangement. Biological information of nodes and edges, such as gene name and annotation, can be easily retrieved in the interactive user interface in Cytoscape.

**Figure 2.** Subgraphs of highly variable genes in the pangenome network of 5 pathogenic *E. coli* strains (manually arranged). (a) a cluster of flagellar genes. (b) a cluster containing outer membrane protein-coding genes. (c) a cluster of genes responsible for biosynthesis of the O antigen. (d) another cluster of O antigen-related genes. Green, blue, red nodes and edges denote reference-specific, shared, and query-specific genes and gene adjacencies, respectively. Size of nodes and thickness of edges indicates their weight (occurrence frequency). Numbers alongside shared genes are their indexes in the representative gene set.

**Figure 3.** Two subgraphs of the pangenome network of *E. coli* constructed from 760 metagenomes (manually arranged). (a) a cluster of flagellar genes. (b) a cluster of genes containing MGEs. Green, blue, red nodes and edges denote reference-specific, shared, and query-specific genes and gene adjacencies. Triangles represent MGEs. Size of nodes and thickness of edges indicates their weight

1  
2  
3  
4 (occurrence frequency). Numbers alongside shared genes are their indexes in the representative  
5 gene set.  
6

7 **Figure 4.** Number of subnetworks in pangenome networks derived from varying sizes of recruited  
8 assemblies. The x-axis indicates total length of recruited assemblies for each sub-dataset and the  
9 y-axis represents the number of subnetworks in the pangenome network derived from each sub-  
10 dataset. The curve was fitted for the scatters using the ‘loess’ smoothing method in R[47]. The  
11 shaded area displays the 95% confidential intervals of the curve. Axes are log2-transformed.  
12  
13  
14  
15  
16  
17  
18  
19

## 20 Additional information

21  
22  
23 **Supplementary Figure S1.** Another cluster of genes containing MGEs, flanked by different shared  
24 genes on different *E. coli* genomes (manually arranged). Green, blue, red nodes and edges denote  
25 reference-specific, shared, and query- specific genes and gene adjacencies, respectively. Triangles  
26 represent MGEs. Size of nodes and thickness of edges indicates their weight (occurrence  
27 frequency). Numbers alongside shared genes are their indices in the representative gene set, and  
28 numbers in parentheses indicate loci of these genes in the reference genome.  
29  
30  
31  
32  
33

34 **Supplementary Figure S2.** Examples of arrangement determined by the algorithm. (a)  
35 arrangements for shared nodes (blue) and reference-specific nodes (green). (b-e) arrangements for  
36 query-specific nodes (red).  
37  
38  
39

40 **Supplementary Table S1.** Metadata of isolate genomes used in this study.  
41

42 **Supplementary Table S2.** Statistics for the 5 mock metagenomic datasets.  
43

44 **Supplementary Table S3.** Tables of nodes and edges in the 5-*E. coli*-genome pangenome network  
45 and the 760-metagenome pangenome network.  
46  
47  
48

49 **Supplementary File S1:** Texts for, 1) steps for constructing pangenome networks, 2) steps for  
50 installing the plug-in and visualizing pangenome networks in Cytoscape.  
51  
52

53 **Supplementary File S2:** Texts for, 1) steps for selecting query-specific nodes for arrangement, 2)  
54 Comparison of the reference pangenome network (RPGN) and the query pangenome network  
55 (RPGN), and 3) detailed definitions of conformity and divergence for nodes and edges.  
56  
57  
58  
59  
60  
61  
62  
63  
64  
65

1  
2  
3  
4 **Supplementary File S3:** “5-*E. coli*-genome pangenome network.pdf”, PDF file for *E. coli*  
5 pangenome network derived from five pathogenic *E.coli* strains.  
6  
7

8 **Supplementary File S4:** “760-metagenome pangenome network.pdf”, PDF file for *E. coli*  
9 pangenome network derived from 760 genuine metagenomes.  
10  
11  
12  
13  
14

## 15 Abbreviations

16  
17  
18 *E. coli*: *Escherichia coli*; LPS: lipopolysaccharide; MGEs: mobile genetic elements; *P. copri*:  
19 *Prevotella copri*.  
20  
21  
22  
23  
24

## 25 Ethics approval

26  
27 This study has been approved by the Institutional Review Board on Bioethics and Biosafety  
28 (reference number: BGI-IRB 16017).  
29  
30  
31  
32

## 33 Consent for publication

34  
35  
36 Not applicable.  
37  
38  
39

## 40 Competing interests

41  
42 The authors declare no competing interests.  
43  
44  
45  
46  
47

## 48 References

- 49  
50 1. Tettelin H, Massignani V, Cieslewicz MJ, Donati C, Medini D, Ward NL, et al. Genome  
51 analysis of multiple pathogenic isolates of *Streptococcus agalactiae*: Implications for the  
52 microbial “pan-genome.” *Proc. Natl. Acad. Sci.* [Internet]. 2005;102:13950–5. Available from:  
53 <http://www.pnas.org/cgi/doi/10.1073/pnas.0506758102>  
54  
55 2. Contreras-Moreira B, Vinuesa P. GET\_HOMOLOGUES, a versatile software package for  
56 scalable and robust microbial pangenome analysis. *Appl. Environ. Microbiol.* 2013;79:7696–  
57 701.  
58  
59  
60  
61  
62  
63  
64  
65

3. Zhao Y, Wu J, Yang J, Sun S, Xiao J, Yu J. PGAP: Pan-genomes analysis pipeline. *Bioinformatics*. 2012;28:416–8.
4. Cain AA, Kosara R, Gibas CJ. GenoSets: Visual Analytic Methods for Comparative Genomics. *PLoS One*. 2012;7.
5. Brittnacher MJ, Fong C, Hayden HS, Jacobs MA, Radey M, Rohmer L. PGAT: A multistrain analysis resource for microbial genomes. *Bioinformatics*. 2011;27:2429–30.
6. Fremez R, Faraut T, Fichant G, Gouzy J, Quentin Y. Phylogenetic exploration of bacterial genomic rearrangements. *Bioinformatics*. 2007;23:1172–4.
7. Blom J, Kreis J, Spänig S, Juhre T, Bertelli C, Ernst C, et al. EDGAR 2.0: an enhanced software platform for comparative gene content analyses. *Nucleic Acids Res*. 2016;44:W22–8.
8. Herbig A, Jäger G, Battke F, Nieselt K. GenomeRing: Alignment visualization based on SuperGenome coordinates. *Bioinformatics*. 2012;28:7–15.
9. Pedersen TL, Nookaew I, Wayne Ussery D, Månsson M. PanViz: interactive visualization of the structure of functionally annotated pangenomes. *Bioinformatics* [Internet]. 2017;33:btw761. Available from: <https://academic.oup.com/bioinformatics/article-lookup/doi/10.1093/bioinformatics/btw761>
10. Marcus S, Lee H, Schatz M, Schatz MC. SplitMEM : Graphical pan-genome analysis with suffix skips *BIOINFORMATICS* SplitMEM : Graphical pan-genome analysis with suffix skips. *bioArXiv*. 2014;0–7.
11. Baier U, Beller T, Ohlebusch E. Graphical pan-genome analysis with compressed suffix trees and the Burrows-Wheeler transform. *Bioinformatics*. 2015;32:497–504.
12. Scholz M, Ward D V, Pasolli E, Tolio T, Zolfo M, Asnicar F, et al. Strain-level microbial epidemiology and population genomics from shotgun metagenomics. *Nat. Methods* [Internet]. Nature Publishing Group; 2016; Available from: <http://www.nature.com/doi/10.1038/nmeth.3802>
13. Nayfach S, Rodriguez-Mueller B, Garud N, Pollard KS. An integrated metagenomics pipeline for strain profiling reveals novel patterns of bacterial transmission and biogeography. *Genome Res*. 2016;26:1612–25.
14. Delmont TO, Eren AM. Linking pangenomes and metagenomes: the *Prochlorococcus* metapangenome. *PeerJ* [Internet]. 2018;6:e4320. Available from: <https://peerj.com/articles/4320>
15. Kim Y, Koh I, Young Lim M, Chung WH, Rho M. Pan-genome analysis of *Bacillus* for microbiome profiling. *Sci. Rep*. 2017;7:1–9.
16. Farag IF, Youssef NH, Elshahed MS. Global distribution patterns and pangenomic diversity

- 1  
2  
3  
4 of the candidate phylum “Latescibacteria” (WS3). *Appl. Environ. Microbiol.* 2017;83:1–21.
- 5  
6  
7 17. Cytoscape: An Open Source Platform for Complex Network Analysis and Visualization  
8 [Internet]. [cited 2017 Nov 8]. Available from: <http://www.cytoscape.org/>
- 9  
10 18. Meredith TC, Mamat U, Kaczynski Z, Lindner B, Holst O, Woodard RW. Modification of  
11 lipopolysaccharide with colanic acid (M-antigen) repeats in *Escherichia coli*. *J. Biol. Chem.*  
12 2007;282:7790–8.
- 13  
14  
15 19. Guy L, Jernberg C, Arvén Norling J, Ivarsson S, Hedenström I, Melefors Ö, et al. Adaptive  
16 Mutations and Replacements of Virulence Traits in the *Escherichia coli* O104:H4 Outbreak  
17 Population. *PLoS One.* 2013;8.
- 18  
19  
20 20. Rasko DA, Webster DR, Sahl JW, Bashir A, Boisen N, Scheutz F, et al. Origins of the *E. coli*  
21 Strain Causing an Outbreak of Hemolytic–Uremic Syndrome in Germany. *N. Engl. J. Med.*  
22 [Internet]. 2011;365:709–17. Available from:  
23 <http://www.nejm.org/doi/abs/10.1056/NEJMoa1106920>
- 24  
25  
26 21. Qin J, Li R, Raes J, Arumugam M, Burgdorf KS, Manichanh C, et al. A human gut microbial  
27 gene catalogue established by metagenomic sequencing. *Nature.* Macmillan Publishers Limited.  
28 All rights reserved; 2010;464:59–65.
- 29  
30  
31 22. Le Chatelier E, Nielsen T, Qin J, Prifti E, Hildebrand F, Falony G, et al. Richness of human  
32 gut microbiome correlates with metabolic markers. *Nature.* 2013;500:541–6.
- 33  
34  
35 23. Nielsen HB. Identification and assembly of genomes and genetic elements in complex  
36 metagenomic samples without using reference genomes. *nbt.* 2014;2014:41–5.
- 37  
38  
39 24. Li J, Jia H, Cai X, Zhong H, Feng Q, Sunagawa S, et al. An integrated catalog of reference  
40 genes in the human gut microbiome. *Nat Biotech* [Internet]. 2014;advance on:834–41. Available  
41 from:  
42 <http://dx.doi.org/10.1038/nbt.2942>  
43 [http://www.nature.com/nbt/jour](http://www.nature.com/nbt/journal/vaop/ncurrent/abs/nbt.2942.html#supplementary-information)  
44 [nal/vaop/ncurrent/abs/nbt.2942.html#supplementary-](http://www.nature.com/nbt/journal/v32/n8/full/nbt.2942.html?WT.ec_id=NBT)  
45 [information](http://www.nature.com/nbt/journal/v32/n8/full/nbt.2942.html?WT.ec_id=NBT)  
46 [http://www.nature.com/nbt/journal/v32/n8/full/nbt.2942.html?WT.ec\\_id=NBT](http://www.ncbi.nlm.nih.gov)  
47 [-201408](http://www.ncbi.nlm.nih.gov)  
48 <http://www.ncbi.nlm.nih.gov>
- 49  
50 25. Darmon E, Leach DRF. Bacterial Genome Instability. *Microbiol. Mol. Biol. Rev.* [Internet].  
51 2014;78:1–39. Available from: <http://mmbr.asm.org/cgi/doi/10.1128/MMBR.00035-13>
- 52  
53 26. Whitfield C, Valvano M a. Species-Wide Variation in the *Escherichia coli* Flagellin. *Adv.*  
54 *Microb. Physiol.* 2003;35:135–246.
- 55  
56 27. Reid SD, Selander RK, Whittam TS. Sequence diversity of flagellin (fliC) alleles in  
57 pathogenic *Escherichia coli*. *J. Bacteriol.* 1999;181:153–60.
- 58  
59  
60 28. Beutin L, Delannoy S, Fach P. Sequence variations in the flagellar antigen genes  
61  
62  
63  
64  
65

1  
2  
3  
4 fliC<inf>H25</inf> and fliC<inf>H28</inf> of Escherichia coli and their use in identification  
5 and characterization of enterohemorrhagic E. Coli (EHEC) O145:H25 and O145:H28. PLoS  
6 One. 2015;10.  
7  
8

9  
10 29. Heinrichs DE, Yethon JA, Whitfield C. Molecular basis for structural diversity in the core  
11 regions of the lipopolysaccharides of Escherichia coli and Salmonella enterica. Mol. Microbiol.  
12 1998. p. 221–32.  
13

14  
15 30. Iguchi A, Iyoda S, Kikuchi T, Ogura Y, Katsura K, Ohnishi M, et al. A complete view of the  
16 genetic diversity of the Escherichia coli O-antigen biosynthesis gene cluster. DNA Res.  
17 2015;22:101–7.  
18

19  
20 31. Huynen M, Snel B, Lathe W, Bork P. Predicting protein function by genomic context:  
21 Quantitative evaluation and qualitative inferences. Genome Res. 2000;10:1204–10.  
22

23  
24 32. Delihans N. Impact of small repeat sequences on bacterial genome evolution. Genome Biol.  
25 Evol. 2011;3:959–73.

26  
27 33. Wang D, Li S, Guo F, Ning K, Wang L. Core-genome scaffold comparison reveals the  
28 prevalence that inversion events are associated with pairs of inverted repeats. BMC Genomics  
29 [Internet]. BMC Genomics; 2017;18:268. Available from:  
30 <http://bmcgenomics.biomedcentral.com/articles/10.1186/s12864-017-3655-0>  
31

32  
33 34. Doron S, Melamed S, Ofir G, Leavitt A, Lopatina A, Keren M, et al. Systematic discovery of  
34 antiphage defense systems in the microbial pangenome. Science (80-. ). 2018;1–17.  
35

36  
37 35. Serruto D, Serino L, Massignani V, Pizza M. Genome-based approaches to develop vaccines  
38 against bacterial pathogens. Vaccine. 2009. p. 3245–50.  
39

40  
41 36. Maione D, Margarit I, Rinaudo CD, Massignani V, Scarselli M, Tettelin H, et al.  
42 Identification of a Universal Group B Streptococcus Vaccine by Multiple Genome Screen.  
43 2006;309:148–50.  
44

45  
46 37. Franco AA, Cheng RK, Chung GT, Wu S, Oh HB, Sears CL. Molecular evolution of the  
47 pathogenicity island of enterotoxigenic Bacteroides fragilis strains. J. Bacteriol. 1999;

48  
49 38. Sears CL, Geis AL, Housseau F. Bacteroides fragilis subverts mucosal biology: From  
50 symbiont to colon carcinogenesis. J. Clin. Invest. 2014.  
51

52  
53 39. Scher JU, Sczesnak A, Longman RS, Segata N, Ubeda C, Bielski C, et al. Expansion of  
54 intestinal Prevotella copri correlates with enhanced susceptibility to arthritis. Elife. 2013;

55  
56 40. Laursen BS, Sørensen HP, Mortensen KK, Sperling-Petersen HU. Initiation of protein  
57 synthesis in bacteria. Microbiol. Mol. Biol. Rev. [Internet]. 2005;69:101–23. Available from:  
58 <http://www.scopus.com/inward/record.url?eid=2-s2.0-14844340954&partnerID=tZOtx3y1>  
59  
60  
61  
62  
63  
64  
65

- 1
- 2
- 3
- 4 41. De Boer HA, Hui AS. Sequences within ribosome binding site affecting messenger RNA
- 5 translatability and method to direct ribosomes to single messenger RNA species. *Methods*
- 6 *Enzymol.* 1990;185:103–14.
- 7
- 8
- 9 42. Berwal SK, Sreejith RK, Pal JK. Distance between RBS and AUG plays an important role in
- 10 overexpression of recombinant proteins. *Anal. Biochem.* 2010;405:275–7.
- 11
- 12 43. Zhu W, Lomsadze A, Borodovsky M. Ab initio gene identification in metagenomic
- 13 sequences. *Nucleic Acids Res.* 2010;38.
- 14
- 15 44. Li W, Godzik A. Cd-hit: A fast program for clustering and comparing large sets of protein or
- 16 nucleotide sequences. *Bioinformatics.* 2006;22:1658–9.
- 17
- 18 45. Kent WJ. BLAT - The BLAST-like alignment tool. *Genome Res.* 2002;12:656–64.
- 19
- 20 46. Mende DR, Waller AS, Sunagawa S, Järvelin AI, Chan MM, Arumugam M, et al.
- 21 Assessment of metagenomic assembly using simulated next generation sequencing data. *PLoS*
- 22 *One.* 2012;7.
- 23
- 24 47. R: The R Project for Statistical Computing [Internet]. [cited 2018 Mar 6]. Available from:
- 25 <https://www.r-project.org/>
- 26
- 27
- 28
- 29
- 30
- 31
- 32
- 33
- 34
- 35
- 36
- 37
- 38
- 39
- 40
- 41
- 42
- 43
- 44
- 45
- 46
- 47
- 48
- 49
- 50
- 51
- 52
- 53
- 54
- 55
- 56
- 57
- 58
- 59
- 60
- 61
- 62
- 63
- 64
- 65

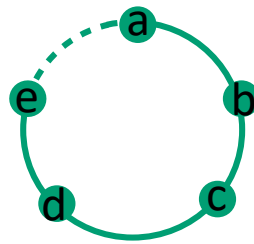
**Table 1. Comparison of several pangenome analysis methods.**

Method	Input	
	Isolate genomes	Metagenomes
GET_HOMOLOGUES [2] and PGAP [3]	Yes	No
GenoSets [4], PGAT [5], PEGR [6], EDGAR [7], GenomeRing [8]	Yes	No
PanViz [9]	Yes	No
SplitMEM10 and a tool introduced by Baier <i>et al.</i> [11]	Yes	No
PanPhlAn [12], MIDAS [13] and a method introduced by Farag <i>et al.</i> [16]	No	Yes
MetaPGN	Yes	Yes



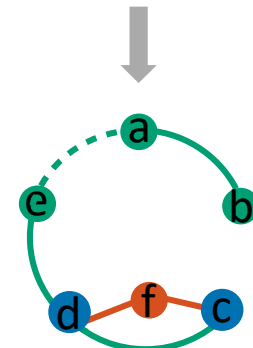
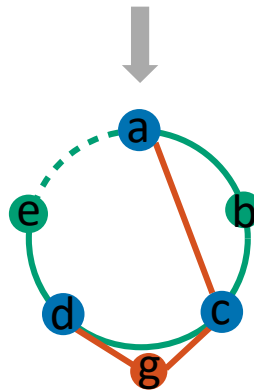
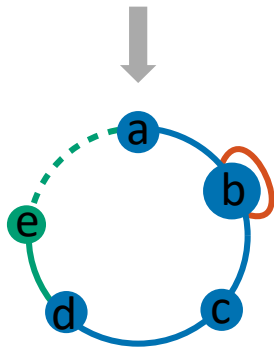
Output			Functionality	
Gene content	Gene-gene adjacency	Network	Biological annotation	Interactive visualization
Yes	No	No	Yes	No
Yes	Yes	No	Yes	No
Yes	Yes	No	Yes	Yes
Yes	Yes	Yes	No	Yes
Yes	No	No	Yes	No
Yes	Yes	Yes	Yes	Yes

## Reference genome

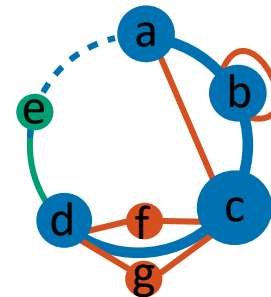


+

## Query assemblies



## Pangenome network



## Node/Edge

- █ reference-specific
- █ shared
- █ query-specific

## Node

## Edge

Name	Freq.	From	Gene	Annotation	...
a	3	S1, S2, Ref	<i>fliA</i>	Sigma factor 28	...
b	2	S1, Ref	<i>fliD</i>	Flagellar capping protein	...
c	4	S1, S2, S3, Ref	<i>fliC</i>	Flagellin	...
d	4	S1, S2, S3, Ref	<i>fliZ</i>	Flagellar assembly chaperone	...
e	1	Ref	Unknown	Unknown	...
...	...	...	...	...	...

Source	Target	Freq.	From	...
a	b	2	S1, Ref	...
b	c	2	S1, Ref	...
b	b	1	S1	...
c	d	2	S1, Ref	...
a	c	1	S2	...
...	...			

Figure 2

[Click here to access/download;Figure;Figure 2.pdf](#)

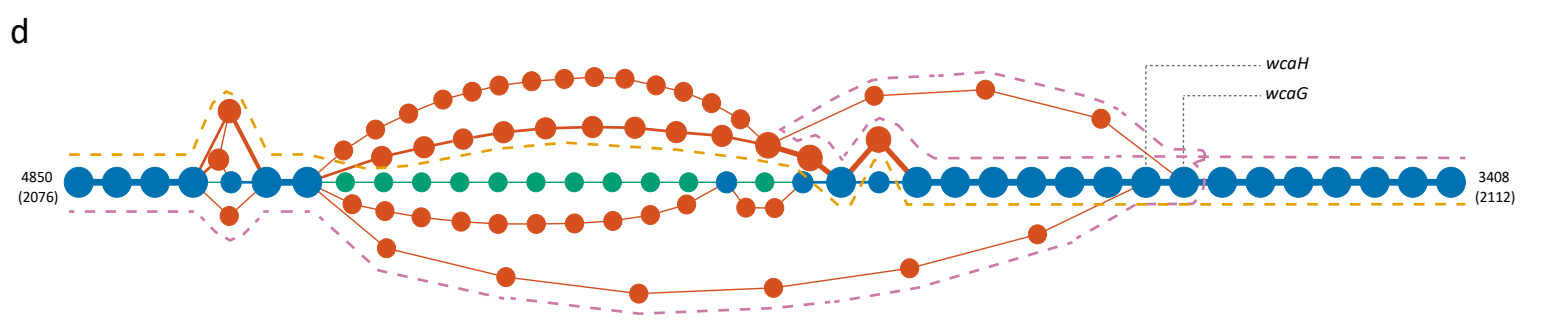
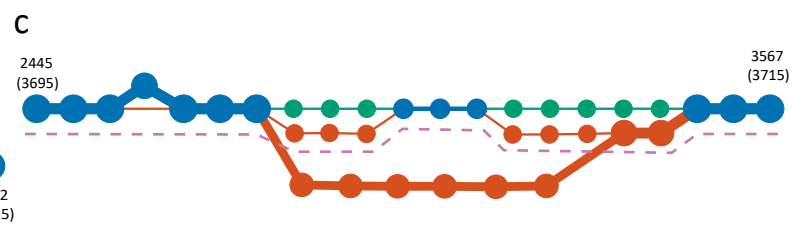
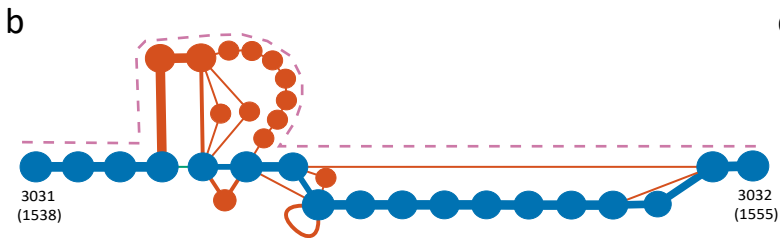
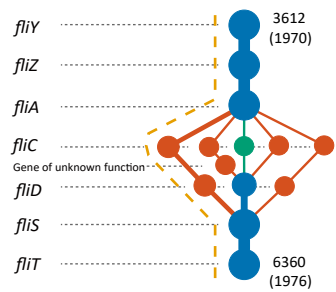
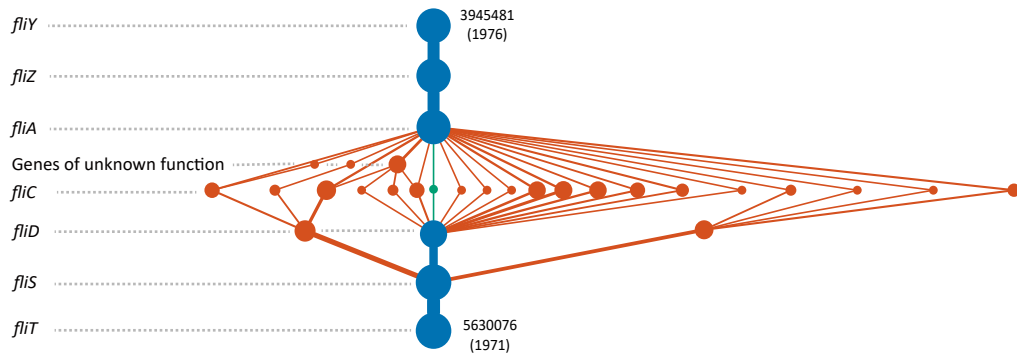


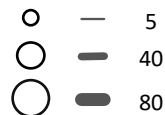
Figure 3 new

[Click here to access/download;Figure,Figure 3 new.pdf](#)



Weight

a



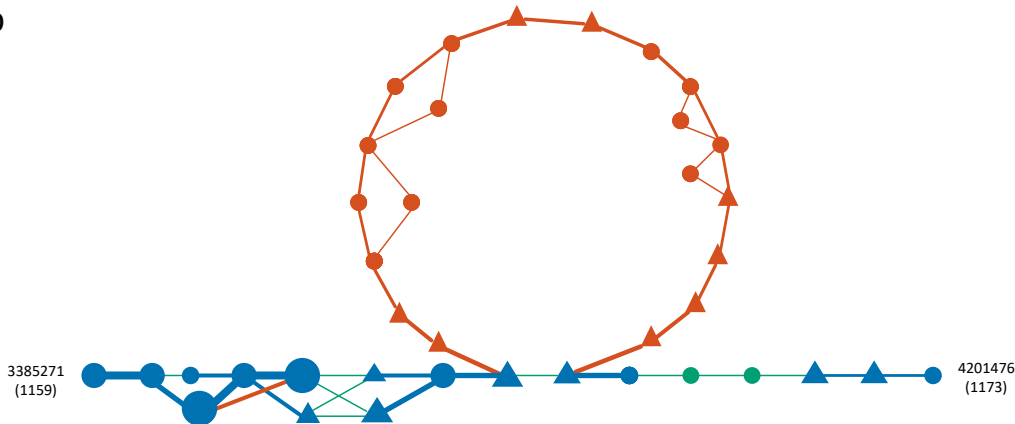
b



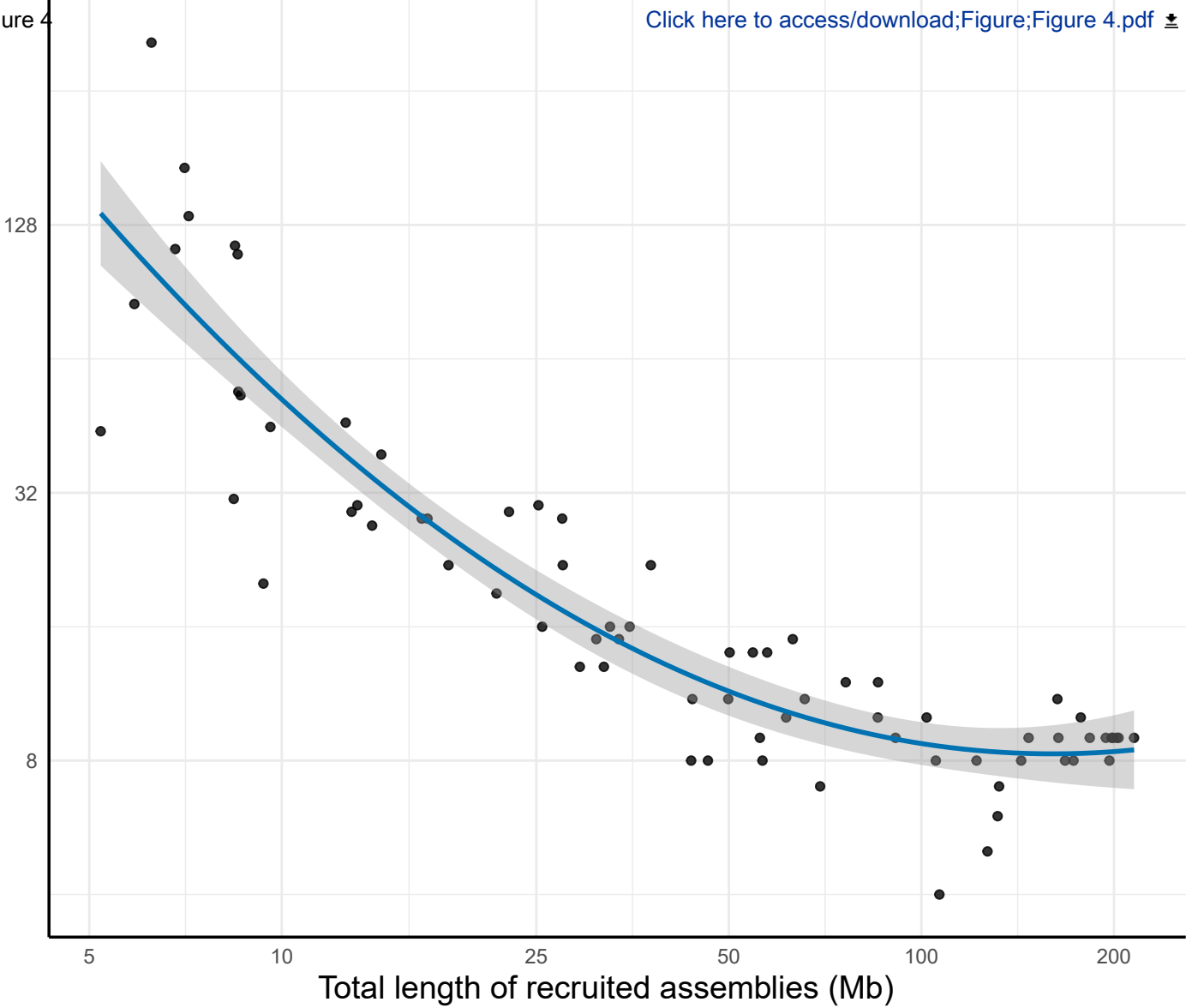
Annotation

▲▲ MGE-related gene

b



Number of subnetworks





Click here to access/download  
**Supplementary Material**  
Supplementary Figure S1.pdf





Click here to access/download  
**Supplementary Material**  
Supplementary Figure S2.pdf





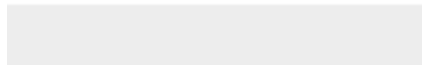
Click here to access/download  
**Supplementary Material**  
Supplementary File S1.docx

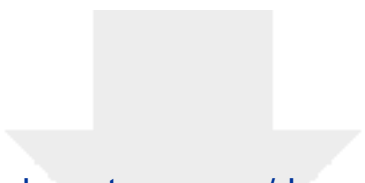







Click here to access/download  
**Supplementary Material**  
Supplementary File S2.docx





Click here to access/download  
**Supplementary Material**  
Supplementary File S3.pdf







Click here to access/download  
**Supplementary Material**  
Supplementary Table S1.xlsx



Click here to access/download  
**Supplementary Material**  
Supplementary Table S2.xlsx



Click here to access/download  
**Supplementary Material**  
Supplementary Table S3.xlsx



[Click here to access/download](#)

**Supplementary Material**

[PBP\\_responses\\_to\\_editor\\_and\\_reviewers.docx](#)

